

Corrosion: Simulating and Rendering

Stephane Merillou

Jean-Michel Dischler

Djamchid Ghazanfarpour

ENSIL - University of Limoges
16 rue Atlantis 87000 Limoges - France

Abstract

Weathering phenomena represent a topic of growing interest in computer graphics, and corrosion reactions are of great importance since they affect a large number of different fields. Previous investigations have essentially dealt with the modeling and rendering of metallic patinas. We propose an approach based on simple physical characteristics to simulate and render new forms of corrosion. We take into account "real world" time and different atmospheric condition categories with experimental data. This allows us to predict the evolution of corrosion over time. The reaction is simulated using a random walk technique adapted to our generic model. For realistic rendering, we propose a BRDF and (color- and bump-) texture models, thus affecting color, reflectance and geometry. We additionally propose a set of rules to automatically predict the preferential starting locations of corrosion.

Key words: Rendering, corrosion, natural phenomena, texturing, BRDF.

1 Introduction

Real-world surfaces are often covered by lots of imperfections due to various aging processes. To compute realistic images, it seems important to take into account such processes by adding a time dependence to rendered scenes. Aging and weathering effects can take many different forms such as dust accumulation, patinas, moisture, scratches, erosion, etc. But, only very few studies have been proposed so far in computer graphics. Dusty surfaces were investigated by Blinn [1] and Hsu [12], tarnished surfaces by Miller [20]. Dorsey [7] proposed a model to take into account dirtiness brought by flow processes. In [24], Wong provided a geometry dependent method to represent dust accumulation, patinas and peeling. Weathering of stones has been studied in [8]. Recently, we introduced a technique to render individually visible scratches appearing on old surfaces [19].

Usually, corrosion reactions can be divided into two main categories: metallic patinas and rusty layers. Dorsey [6] proposed a first phenomenologic model to render metallic patinas based on a multiple layers ap-



Figure 1: Real corroded surfaces

proach. The surface alterations creating these layers are handled by some specific operators and are controlled by specific spreading techniques. To obtain realistic images, the reflectance and transmission of light through these layers are computed with the Kubelka-Munk model [16]. The modelling of corrosion patterns has been studied by Gobron in [10]. Icart [13] proposed to render oxydation layers appearing on materials by using multiple layers BRDF. Metallic patinas, as investigated in [6], consist of a sort of "protection" layer that avoids "too much" matter loss. It affects nearly only color and reflectance (at the human visible scale). On the other side, metals like iron are affected by corrosion in a sort of "destructive way". Great amounts of matter can be wasted compared to patinable materials (such as copper), in particular, holes can appear on the surface.

In this paper, we propose a model to simulate and render new forms of corrosion that correspond to the second category. Our model affects the geometry of objects ("real holes" resulting from the matter loss can appear), as well as its color and reflectance. In section 2, we propose a brief survey of corrosion. Our model, detailed in section 3, permits in a first step to predict the starting locations of corrosion by defining a set of generic rules. In order to compute the "real" matter loss and to obtain a *plausible simulation*, we use a generic law fitting experimental results given in [14]. Then, we describe our random-walk-

based spreading process, resulting in a “corrosion map” (three overlapping maps: a reflectance map, a color map and height map). The map can be pasted and rendered on the object surface using usual texturing techniques or a more accurate virtual ray tracing technique [5] (this is a general form of texture/bump mapping, taking into account light and view dependence, as well as parallax effects and hidden surface removal on the bumps). The corroded parts reflectance is computed by modifying the parameters of the non-corroded surface BRDF: corroded surfaces are particularly rough and porous, thus greatly affecting the global reflectance (BRDF). This is an important issue in computer graphics since metals are usually shiny, while corrosion is rather not. Color is considered either using an approach based on a table of oxidation materials or empirically using color tables gathered from real-world examples (photos). Section 4 shows results obtained for different corrosion processes and different times (given in years). Finally, we conclude this paper in section 5, and discuss some possible improvements of our method as well as some future works.

2 Physics of Corrosion

2.1 Introduction

Corrosion can be defined as the deterioration of a material against its environment. As outlined by Dorsey [6], corrosion is usually very difficult to model precisely because of the huge amount of different reactions, different conditions and different materials. On a physical point of view, corrosion is an electrochemical process requiring the presence of an electrolyte. This electrolyte (for example a thin layer of water) is present on a metallic surface as soon as a certain humidity level is reached (for iron, it is about 60% in unpolluted atmosphere) [2]. However, this level strongly depends on the presence of atmospheric pollutants. The chemical reactions in the case of iron for example imply the creation of many different oxides (with a great variety of chemical structures) composing rust. These oxides all have their own colors (see examples in table 1), explaining the usually noisy and non-uniform aspect of rust color.

formulation	name	color
$\alpha - FeOOH$	goethite	yellowish
$\gamma - FeOOH$	lepidocrocite	dark yellow
Fe_3O_4	magnetite	black
$\alpha - Fe_2O_3$	hematite	reddish
$\gamma - Fe_2O_3$	maghemite	brown

Table 1: Some rust constituents and their colors

In the previous section we already mentioned that corrosion, and especially atmospheric corrosion can follow

two main scenarios, as depicted on figure 2(a) and (b).

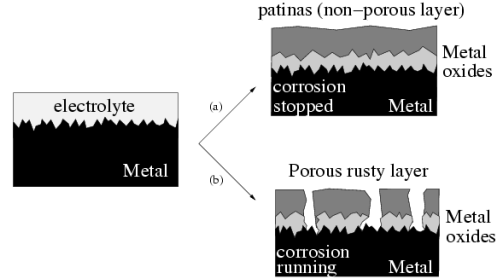


Figure 2: Schematic atmospheric corrosion principle (a) metallic patinas, (b) destructive corrosion.

- (a): products of corrosion create a dense (i.e. non-porous) layer on the surface of the material. In such a case, oxygen and water, required by the chemical corrosion reaction cannot (or nearly not) access to the metal anymore. This means that the corrosion reaction becomes very slow. Such a “protective” layer is called metallic patina [6].
- (b): products of corrosion are concentrated into a porous layer (rust for example). The porosity of such a layer still permits water and oxygen to access to the underlying metal, thus making the chemical corrosion reaction going on. We may call such a layer a “destructive” one. Since the reaction is not stopped, metal is still wasted. In this paper, we are interested in corrosion forms belonging to this category.

2.2 Corrosion: qualitative models

In [9], Fontana established a classification of eight different kinds of corrosion. Dillon [4] noticed that the following four are identifiable by ordinary visual examination. We limited our study to these cases:

- *Uniform corrosion*: corrosive attack over the entire surface area (at least a large proportion). It is one of the most important forms of corrosion. Its rate is nearly constant over the entire surface;
- *Galvanic corrosion* appears when two different materials are coupled in a corrosive electrolyte: the more electrochemically noble is protected while the less noble one tends to corrode at an accelerated rate proportional to the ratio “protected” vs. “corroded” exposed area;
- *Pitting corrosion* is a process which produces localized cavities in the material. It is characterized by a

pitting factor, which is the ratio of the deepest cavity by the mean thickness loss. A pit may be initiated by a localized surface defect or a local material composition variation.

- *Crevice corrosion* is often due to a differential aeration: that is, a sudden difference of the oxygen accessibility over two parts of the same material. Corrosion is greater onto the oxygen hardly accessible parts. The mechanisms of crevice corrosion and pitting corrosion are often similar [2].

The other forms: *intergranular corrosion*, *dealloying*, *erosion corrosion* and *stress corrosion* occur in more specific cases (in specific alloys or under mechanical stress ...). The corrosion observable on real surfaces can be a combination of these different processes.

A metallic surface is never perfectly clean in real world. For example, very thin grease layers can slow down the corrosion process. Impurities can also occur, thus resulting in local galvanic corrosion. Microgeometric surface details (such as scratches) are also important: their mechanical creation can remove dirtiness layers and their shape introduces a localized differential aeration, thus increasing the corrosion rate. Other factors are imaginable. Figure 1 shows real photographs of corroded surfaces corresponding to the common cases described above: uniform corrosion on a saw, pitting corrosion on one side of the scissors, galvanic corrosion preferentially affecting the welding points of the metallic frame. The last photograph shows on a key that corrosion can start everywhere onto an object (not only into the groove which is mechanically stressed and which retains water).

2.3 Quantification of corrosion

The kinetic of atmospheric corrosion reactions is usually evaluated by a “corrosion rate” giving the amount of wasted material over time per unit area¹. A generic analytical estimation of this rate remains actually impossible since it is necessary to take into account a very large number of different parameters (exact material composition, surface state, exact atmospheric conditions, pollution, etc). Fortunately, sufficient estimations of the steel corrosion rate are given in [14] according to a simple specific atmosphere corrosivity classification. Many common materials are made of steel, so we propose to use this formulation (more precise models or measurements naturally may still be used with our technique). Table 2 shows the mean corrosion rate of steel for different “simple” atmosphere categories.

¹An other expression of the corrosion rate can be given in thickness loss. These different units are linked together by the material density.

Atmosphere corrosivity	first year	10 first years	mean rate stationary
very low	<10	<5	<0.8
low	10-200	5-40	0.8-12
medium	200-400	40-100	12-50
high	400-650	100-250	50-150
very high	650-1500	250-750	150-700

Table 2: steel corrosion mean rate ($g/m^2/year$) vs atmosphere corrosivity [14] as a function of time.

These values permit us to estimate the amount of wasted matter according to a certain time (given in years). By computing this amount for different times (e.g. for 1, 5, 10, 20 and 30 years), the following equation (its coefficients are given in table 3) permits the experimental results of table 2 to be well matched [17]:

$$w(t) = k * t^n$$

w is the corroded weight per unit area, k and n are constants depending on the different conditions, t is the time given in years. The values of k and n , derived from table 2, are shown in table 3.

corrosivity	lost weight
very low	$w = 5.5 * t^{0.565}$
low	$w = 100.4 * t^{0.441}$
medium	$w = 274.6 * t^{0.516}$
high	$w = 477.4 * t^{0.638}$
very high	$w = 954.8 * t^{0.789}$

Table 3: Analytic functions to evaluate corrosion rate by evaluating the lost weight in ($g/year$)

3 Modeling and Rendering corrosion

In the following two subsections, we first describe the automatic selection of corrosion starting points (the amount n_0 of points is given by the user while their locations are computed automatically). The location depends on the type of corrosion, on the global scene geometry, on user-defined characteristics such as “dirtiness” (i.e. grease or other impurities) and on surface microgeometry imperfections (scratches for example). All of these characteristics have a noticeable influence on the spread of corrosion. Then, in the next subsection, we describe the corrosion simulation process that is based on a random-walk taking into account the previously described corrosion rates. Rendering issues are also discussed.

3.1 Starting points of corrosion

We assume that the scene is composed of different metallic objects and that the user has indicated how “noble” (from an electrochemical point of view, see [11]) these objects are with respect to each other. We need to determine what objects’ zones are likely to be affected more or less importantly by corrosion according to: 1. their own “internal” characteristics and 2. their “external” conditions into the scene.

First, for each metallic object, the user selects the amount n_o of starting points. This amount actually depends on many parameters that would be difficult to determine accurately and physically (for example, measuring the exact number and locations of impurities included into the surface turns out to be very hard). We assume that the object is given in the form of a mesh. We must determine where the n_o starting points are preferentially distributed on the surface, that is, the probability of a face to get a starting point or not (or even multiple points). Initially each face F_i has a probability coefficient p_i equal to $Area(F_i) / \sum Area(F_i)$. This means that all faces have a probability proportional to their surface area (infinitesimal surface elements are equiprobable). These probability coefficients are modified by the two previously mentioned conditions (internal and external). Concerning internal conditions, and because there is no simple way to physically quantify micro-structural imperfections, we empirically propose to use two new coefficients (both are simply “painted” like textures onto the surfaces by the user):

- a microstructure imperfections factor $k_{str,i}$ ($k_{str,i} > 1$), used to increase the coefficient p_i of each face that contains a microstructural defect (for example a scratch [19]),
- a coefficient $k_{gr,i}$ ($k_{str,i} < 1$) used to decrease the coefficient p_i for each face that is covered by a “greasy layer” (greasy layers usually hinder and prevent from corrosion).

Concerning external conditions, the p_i coefficients are modified according to the global scene and object geometry as follows:

- Two objects are in contact (collision) with each other. Galvanic corrosion occurs (see figure 3): the most noble will not be affected and all of its p_i are simply set to zero. Note that we do not consider cases with more than two objects in collision, since such cases are more difficult to handle. Corrosion affects the less noble object and preferentially starts on the faces F_i that are in contact with the noble object. These faces are computed and their probability

coefficient p_i is increased by a factor k_{ext} (see below, for the value of this coefficient). In addition, as outlined in section 2.2, corrosion occurs at an accelerated rate. The acceleration factor is equal to the “protected material” vs. “corroded material” exposed area ratio.

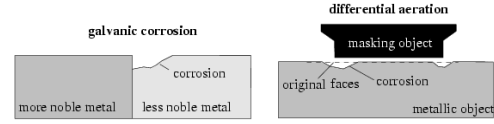


Figure 3: Galvanic corrosion and differential aeration corrosion principles

- The object is isolated: in this case, we need to compute the differential aeration (see figure 3) to determine preferential starting points. Distances between its faces and other object faces are computed. The coefficient p_i of a face F_i is increased by k_{ext} as soon as the proportion of solid angle corresponding to near faces (below a given distance, for example 1 mm) varies strongly with respect to the corresponding proportion of solid angle of neighboring faces. Imagine a pipeline coming out of a wall: the faces of the pipeline close to the wall are characterized by an important variation of the aeration (proportion of solid angles representing far and near objects) due to the presence of the wall.
- Isolated metallic objects (no collision and no significant differential aeration) are affected by uniform corrosion, i.e. all coefficients p_i remain unchanged.

Once all faces F_i of all objects have their own probability coefficient p_i given by

$$p_i = p_{i,initial} * k_{str,i} * k_{gr,i} * k_{ext}$$

(these values are normalized such that their sum equals 1), starting points simply can be selected randomly according to these coefficients: first, a face is randomly selected (according to its probability coefficient), then a point is randomly chosen inside. The coefficients k_{ext} , $k_{str,i}$, $k_{gr,i}$ are selected by the user and allow him to influence the apparition of corrosion on non-preferential parts. With a very important value of k_{ext} and $k_{str,i}$ (for example a factor of 50-100), corrosion will always only start on preferential locations. When all coefficients are set to 1, then corrosion appears equiprobably on all parts. As outlined by Mullins in [21], the locations of corrosion reactions are indeed random functions of time and position, so that their effect on the overall surface can be considered as a classical “white noise” source.

3.2 Computing the corrosion-map

Corrosion processes influence geometry, colors and reflectance of surfaces (see photos of figure 1). It is necessary to combine these three aspect components in order to build a realistic phenomenological model. Our approach consists in simulating the corrosion process on a “thick plate” (corrosion map), then mapping this plate onto the object. Mapping can be performed either using a texel-like approach [15] or, if the thickness is low enough with respect to the entire surface, a bi-directional texture function based on virtual ray tracing [5]. The latter (extending usual texture/bump mapping) is the approach that we used for our examples (corroded thickness is low enough with respect to the surfaces). Our spreading model could allow us to correct mapping distortions in a similar way as in [23] in the case of reaction diffusion processes. Indeed, the corrosion is also a sort of diffusion process. The technique would consist in taking into account the local surface curvature to spread across multiple pixels instead of only one (note that these pixels then must count for only one in the evaluation of the amount of lost weight). Another solution would consist in performing the corrosion spread simulation directly onto the surface, as it has also been proposed in the framework of reaction-diffusion in [22]. However, we not yet implemented such techniques for the sake of simplicity in particular since our visual results did not require it.

The starting points of corrosion that we have previously computed are placed onto the corrosion map using an inverse mapping transformation. With these starting points, the spreading process can be run onto the map. Each corrosion map pixel contains following information: a color, a porosity coefficient, a roughness coefficient (both are used for the BRDF) and an elevation decreasing according to the spread of corrosion (if the elevation falls under a certain limit, corresponding to the real thickness of the object, we consider that there is a hole). The specific color is computed according to table 1 or according to an example photo. The porosity and roughness coefficients are used to modify the BRDF model with similarity to [18] (see section “*affecting roughness and porosity*”).

corrosion spread

We consider that the corrosion map has a unit size of $1 m^2$ (by mapping it, it will correspond to the “real” object area). The principle now simply consists of spreading the corrosion using a random walk technique. The difficulty however, is that the spread occurs either into the volume or onto the surface (see figure 4), while it is important to respect the corrosion rates given in table 2.

The user indicates the real thickness corresponding to the object (for example in mm). This is also the thickness

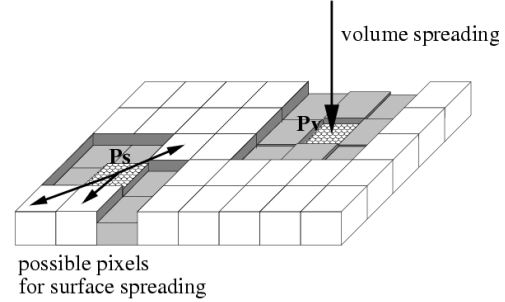


Figure 4: Different spreading cases.

of the corrosion map which is initialized with the previously computed n_0 corrosion starting points. Initially, these pixels are marked as corroded. The first step consists of computing a list l_{cp} of “already” corroded pixels. In this list, we randomly select one pixel p_s having at least one non-corroded 8-connected neighbor (see figure 4) and one pixel p_v having all its neighbors corroded. Then, the corrosion spreading process is applied to p_s by randomly choosing one of its non-corroded neighboring pixels. The latter is marked as corroded: its color is selected from a table, its porosity and roughness affected, and its height is decreased by δ (see below). Concerning p_v (if existing), the spreading process goes directly in depth, that is, we decrease the depth value by δ . Note that δ depends for each pixel on the local amount of already corroded matter. So, the δ of p_v is not necessarily the same as the previous one (p_s). If the corrosion map pixel’s height is greater than the map thickness a hole appears (the concerned pixels can no longer be chosen). Newly corroded pixels are added to the list l_{cp} . The actual lost weight is calculated and compared to the weight to be reached (given by table 3 according to the chosen time). Unless the wasted weight does not reach the required value, the process is re-iterated eventually with an addition of new starting points by a value which can be randomly taken between 0 and n_0 (to account for surface state variations with time). The lost weight is computed by evaluating the lost volume per newly corroded pixel and by using the density of iron (about $\rho_{iron} = 7.8 g/cm^3$). The pixel surface is $S_p = (100 cm/Map Resolution)^2$ and its volume is $\delta * S_p$.

calculating δ

If the corrosion was purely uniform onto the entire surface, at each spreading step, it would be easy to find the lost thickness (e.g. the same δ for all pixels) using table 3. However corrosion does not affect all the pixels of the map at the same time as induced by the use of a time dependent spreading technique with preferential starting points. Thus, we need for each pixel to evaluate a specific

δ . This is achieved by calculating for each pixel a “local corrosion time” t_{local} : knowing the lost thickness of this pixel (this is the pixel height in the corrosion map), we can calculate the equivalent lost weight w_{eq} :

$$w_{eq} = \text{pixel height} * S_p * \rho_{iron}$$

Solving equations of table 3 in t leads to

$$t_{local} = e^{(1/n)*\ln(w_{eq}/k)}$$

The mean weight of matter to be lost at this time for this pixel is

$$\Delta w = w(t_{local} + 1) - w(t_{local})$$

which corresponds to a mean height loss of

$$h_l = \Delta w / (\rho_{iron} * S_p)$$

h_l should correspond to δ , however a real surface cannot be handled in such a constant way as it might contain impurities or inclusions locally decreasing or increasing corrosion rates. Since it is not actually possible to obtain all of this information, we empirically choose to add randomness by selecting δ as a random value around h_l . We note that in the particular case of pitting corrosion, δ can be increased by a physically defined factor called “pitting factor” that is the ratio between the maximum depth of a pit and the average thickness loss [17]. Since we did not dispose of experimental data concerning this value, we empirically used 10 in our examples which gave visually satisfactory results.

Affecting roughness and porosity

On non-corroded parts, we use the Cook and Torrance BRDF model [3] for iron. On corroded parts, we use the model described in [18] which accounts for both porosity and roughness. Porosity is empirically chosen to be 80%, since rust is a very porous matter [17]. As described in [18], porosity increases the diffuse vs. specular coefficients (indeed rust is not shiny as opposed to iron). Roughness was augmented by a factor of about 3, which approximately corresponds to the values that we measured using a HommelWerke HommelTester T2000: a profile and roughness measurement tool (see figure 5).

Figure 6 illustrates the corrosion spread (changes of color and geometry) using the previously described random walk algorithm with 5 starting points and for different corrosion times, under medium corrosivity. The thickness of the map is 1.2 mm. During the corrosion process new starting points have been randomly added.

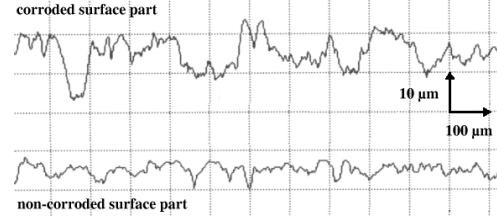


Figure 5: Roughness measurements of a corroded part (top) and a non-corroded part (bottom) of the same surface. For both figures the scale is the same.

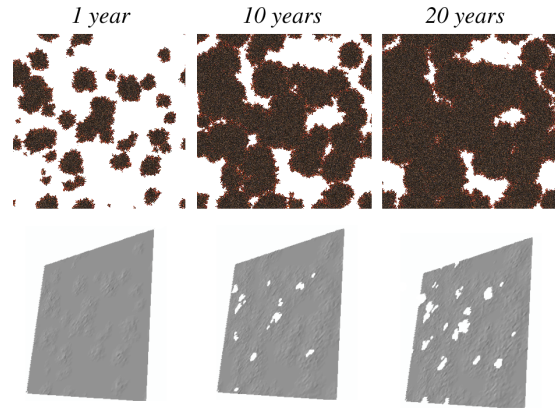


Figure 6: Full corrosion spread using our modified random walk (holes begin to appear up to 5 years)

4 Results

In this section, we illustrate some of the previously described corrosion forms. First a galvanic corrosion has been computed: a screw on a more noble metallic rod. Our algorithm detects that the screw does corrode at an accelerated rate. On the left-top of figure 7: corrosion starts on the invisible parts of the screw and propagates preferentially from the screw border to its center. A real photograph of the same kind of scene is also provided (left-bottom part). The spreading is done under high corrosive atmosphere during 5 years. Another kind of prediction that we introduced in this paper is based on differential aeration. On figure 7-right, a metallic pipe comes out of a wall. Oxygen cannot access to the parts of this pipe that are “into” the wall. Corrosion starts preferentially in the close neighborhood of the wall, and just into the wall hole. To render this image we choose a medium corrosivity and show the result for a 8 years period.

On figure 8, corrosion greatly affects the geometry of the tool. See in particular its sharp edge and its shadows (conditions are a medium corrosivity during 25 years with 20 starting points).

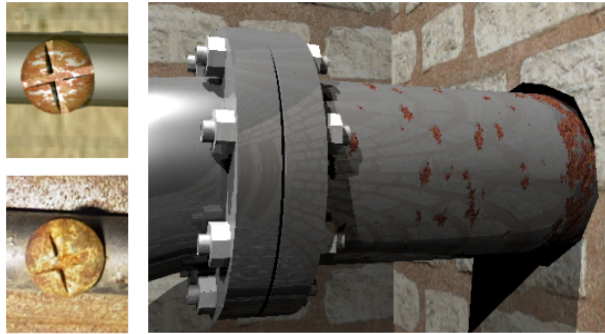


Figure 7: Prediction of corrosion spreading - Galvanic corrosion (left) - Differential aeration (right)

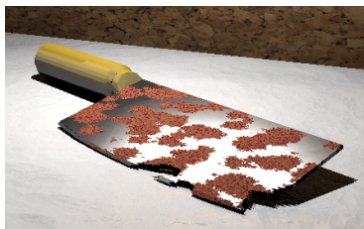


Figure 8: Affected geometry of a tool

Figure 9 shows the differences obtained between pitting (the first line of pictures) and uniform corrosion (the second line). On a same column of this figure, the amount of wasted matter is the same (due do identical corrosivity and time) but in the case of pitting corrosion the spread process goes mainly into the object, thus greatly affecting the object geometry (“holes” creation). The uniform corrosion spread is mainly a surface one. From left to right, time is 1, 5 and 10 years under very high corrosivity (industrial marine environment for example). Pitting points have been randomly chosen onto the corroded surface.

Finally, figure 10 illustrates that corrosion can be at the origin of great amounts of wasted matter. The left part is a real highly corroded wheelbarrow, the right part is a corresponding rendered image (conditions are a high corrosivity during 12 years with 20 starting points, thickness of the metal sheet is 4 mm).

5 Conclusions and Future Work

We have proposed a first phenomenological model addressing the simulation and rendering corrosion (rust) of metals (especially steels), using an approach based on experimental data. The model affects color, reflectance and geometry. A first attempt of a physically based automatic prediction has also been proposed to localize the beginning of corrosion reactions. Though our model depends on many parameters (yet it is very simplified and thus is

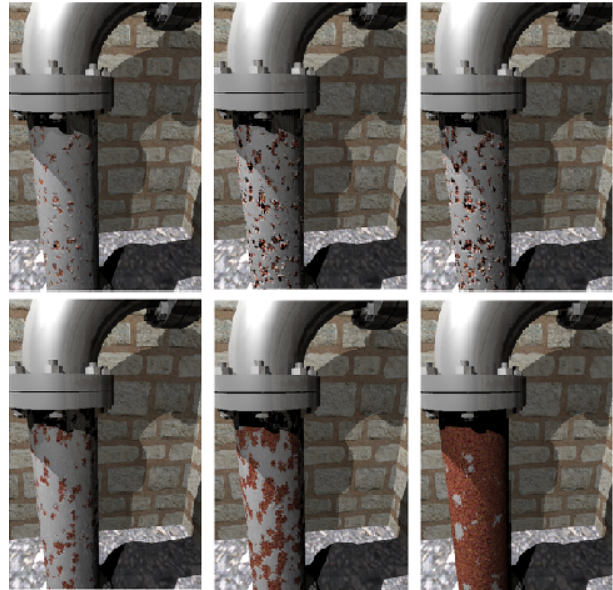


Figure 9: Pitting corrosion (top) compared to uniform corrosion (bottom)

not a fully physical model), they remain intuitive enough to be used in computer graphics applications, allowing for a good control of the aspect of corroded surfaces. However, the model is limited to the corrosion “attack” itself, while we have not considered other accompanying effects. Indeed, often also non-corroded parts are affected by time. Pollution adherence, rust transport and other stresses also create aspect variations (this explain the wheelbarrow color differences on the figure 10). It should be possible to use the technique developed in [7] for transport simulation. The corrosion BRDF may also be improved in several ways: in our future works, we intend to take into account multiple layers as well as sub-surface scattering. Also, mechanical properties of materials need to be studied in order to predict for example the fracture of rusty objects when corrosion has removed enough matter. This can lead us to a complete time dependent system to predict the appearance of entire scenes after several years under different atmospheric conditions.

References

- [1] JF Blinn, “Light Reflection Functions for Simulation of Clouds and Dusty Surfaces”, *Computer Graphics* 16(3), pp. 21-29, ACM SIGGRAPH, 1982.
- [2] WD Callister, “Materials Science and Engineering: An Introduction”, John Wiley and Sons Inc. New-York, 1994.



Figure 10: Comparison between a real photograph and a render image of a corroded wheelbarrow

- [3] RL Cook, KE Torrance, "A Reflectance Model for Computer Graphics", *Computer Graphics* 15(3), pp. 307-316, ACM SIGGRAPH, 1981.
- [4] CP Dillon, "Forms of Corrosion, Recognition and Prevention", NACE International, Houston, 1982.
- [5] JM Dischler, "Efficiently Rendering Macro Geometric Surface Structures with Bi-Directional Texture Functions", *Eurographics Workshop on Rendering*, pp. 169-180, Vienna, 1998.
- [6] J Dorsey, P Hanrahan, "Modeling and Rendering of Metallic Patinas". *Computer Graphics* pp. 387-396, ACM SIGGRAPH, 1996.
- [7] J Dorsey, H Pedersen, P. Hanrahan, Flow and Changes in Appearance. *Computer Graphics*, pp. 411-420, ACM SIGGRAPH, 1996.
- [8] J Dorsey, A Edelman, H Jensen, J Legakis, H Pedersen, "Modeling and Rendering of Weathered Stone", *Computer Graphics*, pp. 225-234, ACM SIGGRAPH, 1999.
- [9] MG Fontana, "Corrosion Engineering", McGraw Hill, New-York, 1986.
- [10] S Gobron, N Chiba, "3D Surface Cellular Automata and their Applications", *Journal of Visualization and Computer Animation*, (10), pp. 143-158, 1999.
- [11] HP Hack, D Taylor, "Metals Handbook", 9th Edition, Vol 13, ASM Metals Park, 1987.
- [12] S Hsu, T Wong, "Simulating Dust Accumulation", *IEEE Computer Graphics and Applications* 15(1), pp. 18-22, 1995.
- [13] I Icart, P Arques, "A Physically-based BRDF Model for Multilayer Systems with Uncorrelated Rough Boundaries", *Eurographics Workshop on Rendering* 2000.
- [14] ISO Norm 9223, "Corrosivity Classification".
- [15] JT Kajiyia, TL Kay, "Rendering Fur with Three Dimensional Texture", *Computer Graphics* 23(3), pp. 271-280, ACM SIGGRAPH, 1989.
- [16] G Kortum, "Reflectance Spectroscopy", Springer-Verlag, New-York, 1969.
- [17] D Landolt, "Corrosion, chimie de surface des metaux", Presses Polytechniques et Universitaires Romandes, Alden Press, Oxford, 1993.
- [18] S Merillou, JM Dischler, D Ghazanfarpour, "A BRDF Post-Process to Integrate Porosity on Rendered Surfaces", *IEEE Transaction on Vizualisation and Computer Graphics*, vol 6(4) oct-dec 2000.
- [19] S Merillou, JM Dischler, D Ghazanfarpour, "Surface Scratches, Measuring, Modeling and Rendering", *The Visual Computer*, vol 17(1), pp. 30-45, 2001.
- [20] G Miller, "Efficient algorithms for local and global accessibility shading", *Computer Graphics*, pp. 319-326, ACM SIGGRAPH 1994.
- [21] WM Mullin, EJ Shumaker, GJ Tyler, "Stochastic Kinetics of Corrosion and Fractal Surface Evolution", *Journal of Corrosion Science and Engineering*, (1)7, 1997.
- [22] G Turk, "Generating Textures on Arbitrary Surfaces using Reaction-Diffusion", *Computer Graphics*, pp. 289-298, ACM SIGGRAPH, 1991.
- [23] A Witkin, M Kass, "Reaction-Diffusion Textures", *Computer Graphics*, pp. 299-308, ACM SIGGRAPH, 1991.
- [24] TT Wong, WY Ng, PA Heng, "A Geometry Dependent Texture Generation Framework for Simulating Surface Imperfections", *Eurographics Workshop on Rendering*, pp. 139-150, 1997.